Electronic Supplementary Material (ESI) for Chemical Communications

Electronic Supplementary Information

Poly(fluorene-thiophene) Donor Tethered Phenanthro[9,10-d]imidazole Acceptor for Flexible Nonvolatile Flash Resistive Memory Devices

Hung-Chin Wu,‡[a] An-Dih Yu,‡[a,b] Wen-Ya Lee,[a] Cheng-Liang Liu,*[c] and Wen-Chang Chen*[a]

[a] *Department of Chemical Engineering, National Taiwan University, Taipei 10617, Taiwan. E-mail: chenwc@ntu.edu.tw*

[b] *Department of Organic Device Engineering and Research Center for Organic Electronics, Yamagata University, Yonezawa, Yamagata 992-8510 Japan.*

[c] *Department of Chemical and Materials Engineering, National Central University, Taoyuan 32001, Taiwan. E-mail: clliu@ncu.edu.tw*

‡ The first two authors contributed equally to this paper

S1. Materials

All commercially available reagents or anhydrous solvents obtained from suppliers were used without further purification. 2,2'-(9,9-dioctyl-9H-fluorene-2,7-diyl)bis(4,4,5,5-tetramethyl-1,3,2-dioxaborolane) (**F**)[S1] and 2-(2,5-dibromothiophen-3-yl)-6,9-dihexyl-1-(4-hexylphenyl)-1H-phenanthro[9,10-d]imidazole (**T-PI**)[S2] were prepared according to literature procedures.

S2. Polymer Synthesis

Poly[2,2'-(9,9-dioctyl-9H-fluorene-2,7-diyl)-alt-2-(2,5-thiophen-3-yl)-6,9-dihexyl-1-(4-hexylphenyl)-1H-phenanthro[9,10-d]imidazole] (**PFT-PI**) was synthesized by Suzuki coupling polymerization as shown in Scheme S1 (see SI). A 3-neck flash connected to a condenser was charged with following materials: a stir bar, diborate monomer (**F**; 310.1 mg (0.48 mmol)), dibromo monomers (**T-PI**; 379.7 mg (0.48 mmol)), tetrakis(triphenylphosphine)palladium(0) ($Pd(PPh_3)_4$; 5.55 mg (4.8 μmol)), and a mixture of toluene and aqueous 2M K_2CO_3 (3/2 volume ratio) with several drops of aliquat® 336. The reaction mixture was refluxed under vigorous stirring for 72 h under a nitrogen atmosphere. The end groups were capped by refluxing for 12 h each with phenyl boronic acid and bromobenzene (both 1.1 equiv. with respect to diborate monomer) before being precipitated into a mixture of methanol and water. The precipitated compound was dissolved into a small amount of THF and then re-precipitated into methanol. The crude product was purified by Soxhlet extraction with methanol, acetone and hexanes and followed by drying at 40 ^{o}C under vacuum to afford a yellow solid (yield: 75 %). ^{1}H NMR (CD_2Cl_2, 400 MHz,): δ = 8.75-8.58 (m, br, Ar H), 8.58-8.38 (m, br, Ar H), 7.82-7.35 (m, br, Ar H), 7.35-6.88 (m, br, Ar H), 6.88-6.68 (br, Ar-H), 2.91 (br, Ar CH_2), 2.80-2.50 (m, br, Ar CH_2), 2.02 (br, Ar CH_2), 1.88-1.55 (m, br, CH_2), 1.55-1.22 (m, br, CH_2), 1.22-0.95 (m, br, CH_2), 0.95-0.30 (m, br, CH_3). Anal. Calcd. for $C_{72}H_{92}N_2S$: C 84.98, H 9.11, N 2.75, S 3.15; found: C 84.65, H 9.28, N 2.72, S 3.43.

S3. Instrumentation

^{1}H-NMR spectra were obtained in CD_2Cl_2 with a Bruker Avance DRX-400 MHz spectrometer. Gel permeation chromatographic (GPC) analyses were performed on a Lab Alliance RI2000 instrument (two column, MIXED-C and D from Polymer Laboratories) connected with one refractive index detector from Schambeck SFD Gmbh. All GPC analyses were performed on polymer/THF solution at a flow rate 1 ml min^{-1} and temperature 40 ^{o}C and calibrated with polystyrene standards. Element analyses were performed with a Heraeus varioELIII-NCSH instrument. Thermogravimetric analysis (TGA) and differential scanning calorimetry (DSC) measurements were performed under a nitrogen atmosphere at a heating rate of 10 ^{o}C min^{-1} using the TA instruments Q-50 and Q-100, respectively.

UV-Vis absorption spectral data were measured with Hitachi U-4100 spectrophotometer. Thin film measurements were collected by spin-coating onto untreated quartz substrate. Cyclic voltammetry (CV) was collected using CHI 611B electrochemical analyzer. A three-electrode cell based on ITO glass working electrode, an Ag/AgCl, KCl (sat.) reference electrode (calibrated vs Fc/Fc^+) and a Pt wire counter electrode was purged with a nitrogen. The electrochemical properties of the polymer films were detected under 0.1 M anhydrous acetonitrile solution containing tetrabutylammonium perchlorate (TBAP) as the supporting electrolyte. The thickness of polymer film was determined with a Microfigure Measuring Instrument (Surfcorder ET3000, Kosaka Laboratory Ltd.).

S4. Computational Methodology

Molecular calculations studied in this work have been performed through Gaussian 03 program package.[S3] Equilibrium ground state geometry and electronic properties were optimized by means of the density functional theory (DFT) method at the B3LYP level of theory (Beckes-style three-parameter density functional theory using the Lee-Yang-Parr correlation functional) with the 6-31G(d) basic set.

S5. Characterization

The position and integration of peak signals of ^{1}H NMR spectrum were consistent with the proposed **PFT-PI** structures. The carbon, hydrogen, nitrogen and sulfur experimental contents of the synthesized **PFT-PI** were all in a good agreement with theoretical contents. TGA showed a decomposition temperature of 415 ^{o}C, implying a high thermal stability. DSC results did not reveal any obvious transition until 300 ^{o}C. As the bulky phenanthro[9,10-d]imidazole side chain moiety was attached, the glass transition temperature was not clearly detectable.[S2] The excellent thermal stability of conjugated **PFT-PI** is expected to be beneficial for device fabrication and meet the requirement of heat resistance in the electronic industry.

S6. Device Fabrication and Measurement

PEN substrate was first pre-cleaned by an ultrasonic cleaning process with water, isopropanol, and acetone successively for 15 minutes each. 30-nm thick Al bottom electrode patterns were deposited by a thermal evaporator at a pressure of 10^{-5} torr with a depositing rate of 1 Å s^{-1}. Then, 8 mg mL^{-1} of **PFT-PI** in chloroform was filtered through 0.22 μm pore size of PTFE membrane syringe filter, spin-coated onto the bottom Al electrode/PEN substrate at 1000 rpm for 60 s and baked at 100 ^{o}C on a hot plate in N_2-filled glove box. Finally, the 30-nm Al top electrodes was deposited and patterned by a metal mask with cross-point device joint area of 0.2 × 0.2, 0.4 × 0.4 and 0.6 × 0.6 mm^2, respectively. The sneak path problem can be overcome by introducing additional control elements between the electrode and memory elements. However, in this work, a single bit-line with several word lines were made (for example, retrieved from 6 bits; a 1 × 6 array for 0.4 × 0.4 mm^2 cross-point device) to demonstrate the **PFT-PI** device for flexible electronics and verify the correct reading of the information. All the electrical characteristics of the fabricated flexible memory devices were measured by a Keithley 4200-SCS semiconductor parameter analyzer using a probe station at room temperature in a N_2-filled glove box. The bottom electrode was grounded during all the electrical measurement with a swept step of 0.1 V.

S7. Reference

[S1] J. Y. Lee, Y. J. Kwon, J.-W. Woo and D. K. Moon, *J. Ind. Eng. Chem.*, 2008, **14**, 810.

[S2] Y.-T. Chang, S.-L. Hsu, M.-H. Su and K.-H. Wei, *Adv. Mater.*, 2009, **21**, 2093.

[S3] Gaussian 03, Revision B.04 Gaussian, Inc., Wallingford, CT 2004.

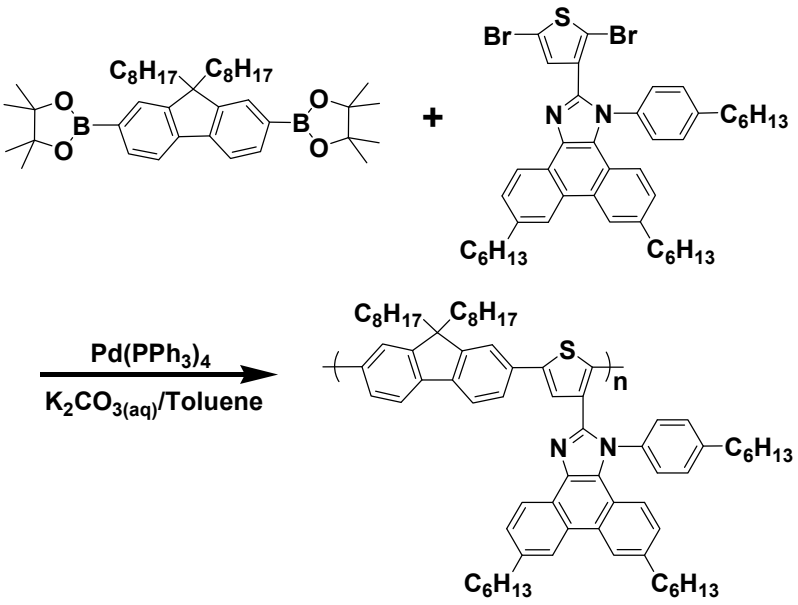

Scheme S1. Reaction scheme of **PFT-PI** conjugated polymer.

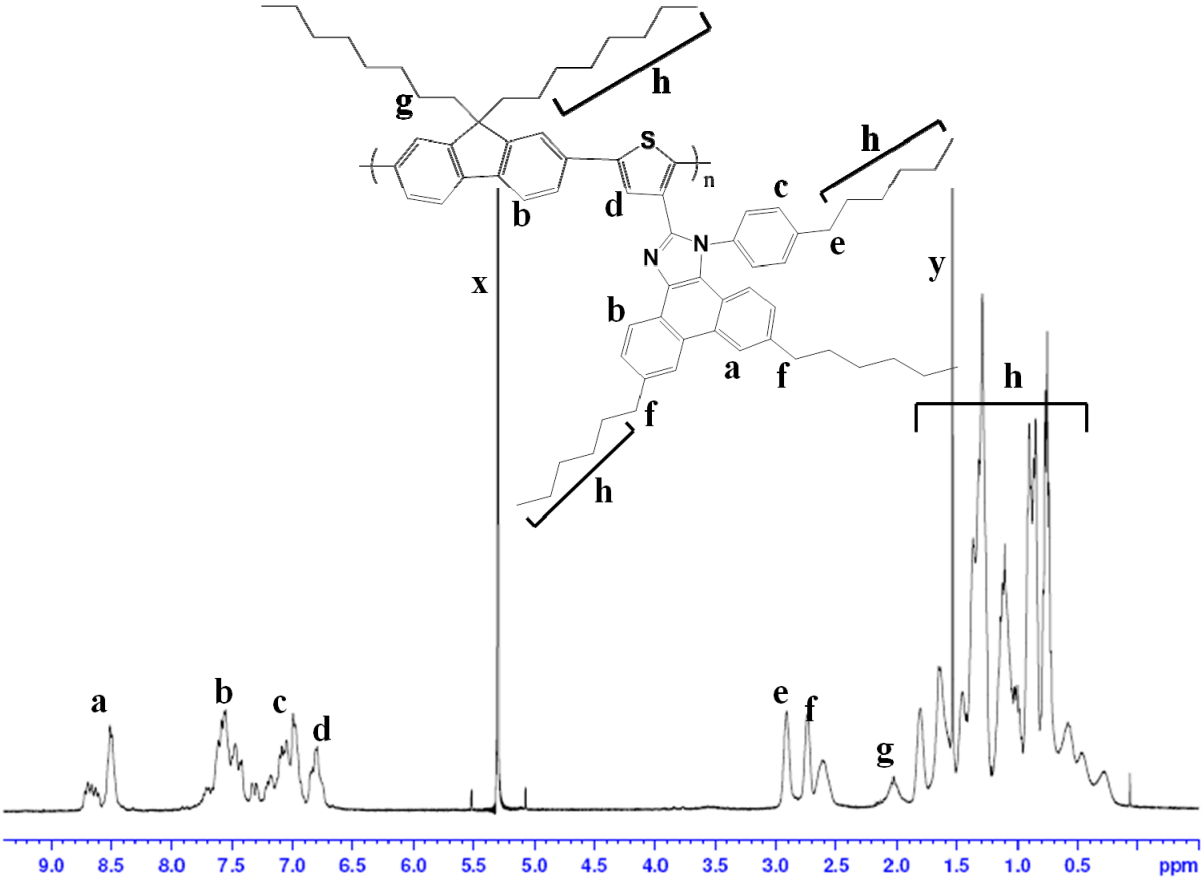

Figure S1. ^{1}H NMR Spectrum of **PFT-PI** in CD_2Cl_2 (x: CD_2Cl_2, y: H_2O).

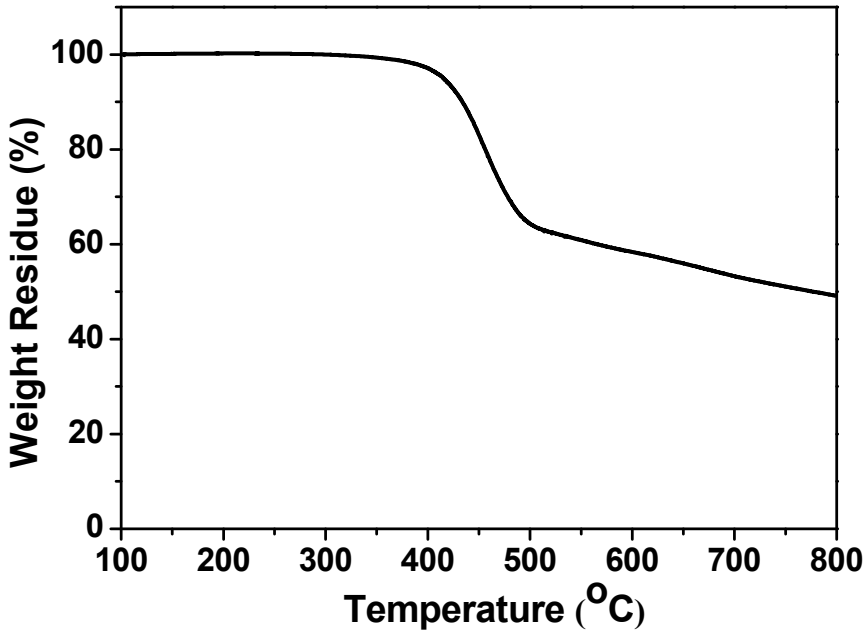

Figure S2. TGA curves of **PFT-PI** at a heating rate of 10 ^{o}C min^{-1} under a nitrogen atmosphere.

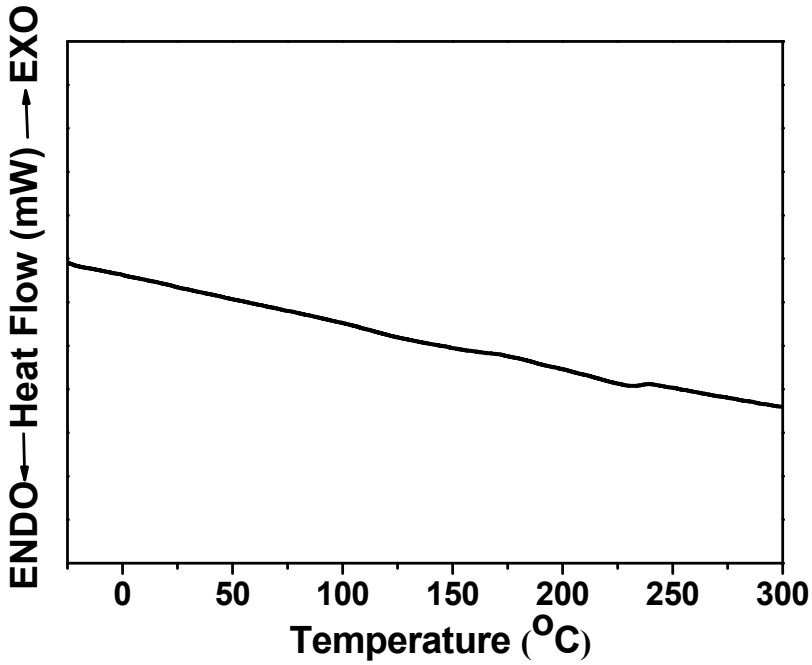

Figure S3. DSC curves of **PFT-PI** at a heating rate of 10 ^{o}C min^{-1} under a nitrogen atmosphere.

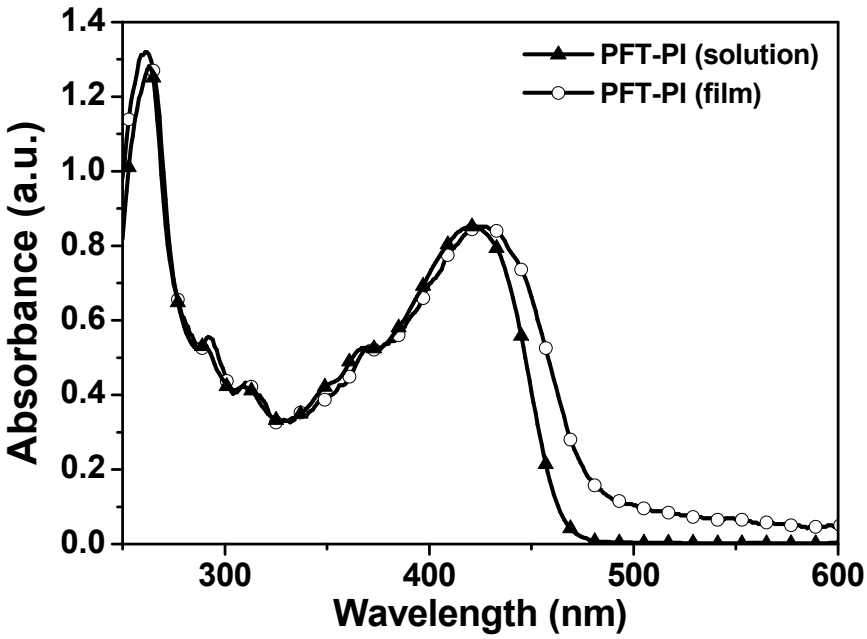

Figure S4. UV-Vis absorption spectra of **PFT-PI** in $CHCl_3$ solution and as a thin film on a quartz substrate.

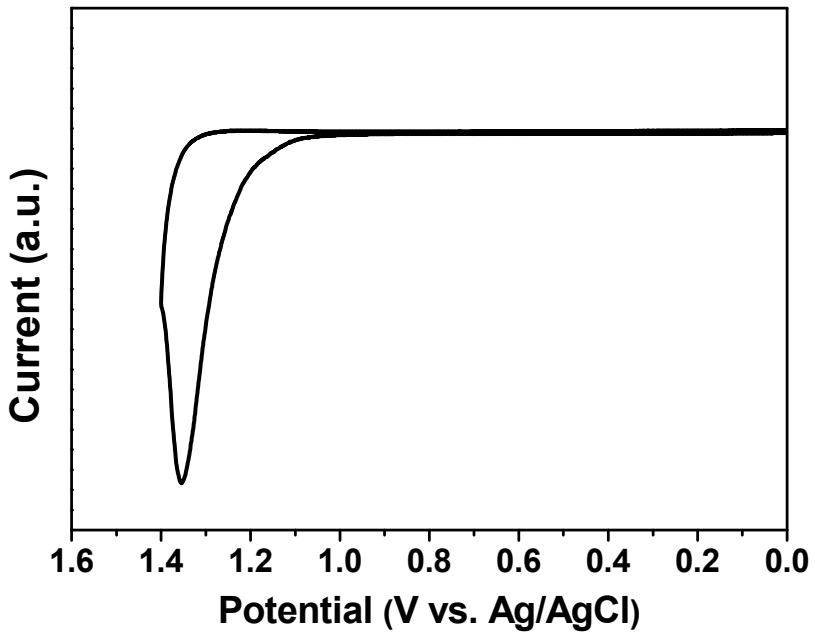

Figure S5. Cyclic voltammogram of the **PFT-PI** thin film spin-coated onto an ITO glass substrate in 0.1 M TBAP/acetonitrile solution at a scan rate of 100 mV s^{-1}.

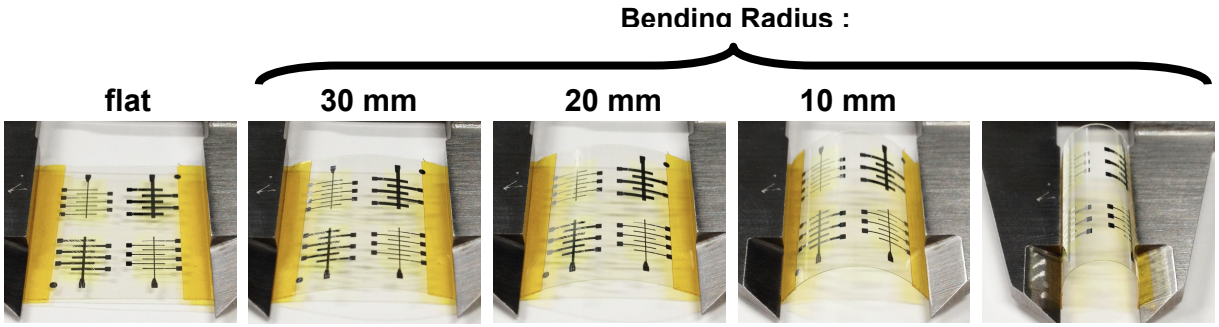

Figure S6. PFT-PI memory device on flat and various bending conditions.

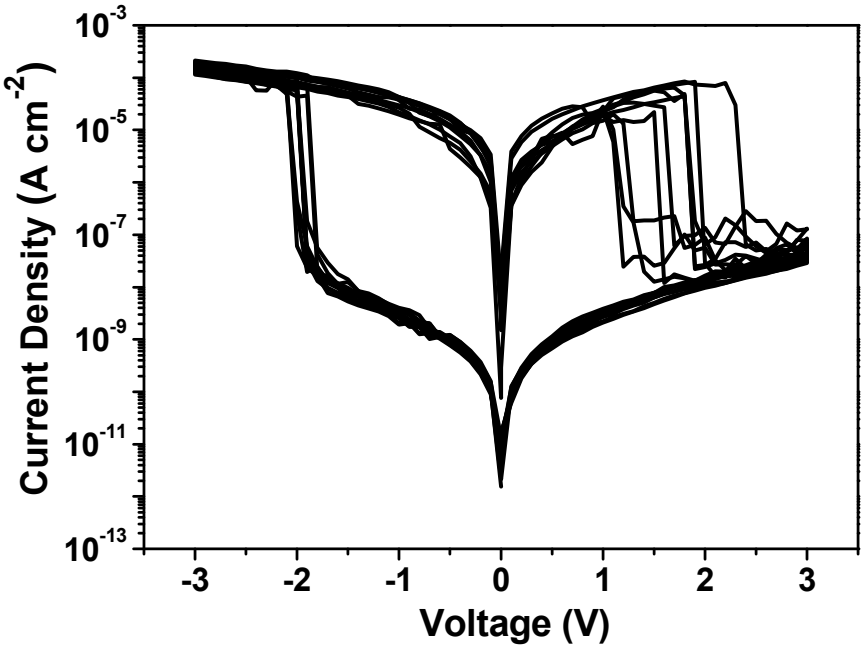

Figure S7. Current density-voltage (*J*-*V*) characteristic of the flexible **PFT-PI** memory device on successive scan under the flat condition.

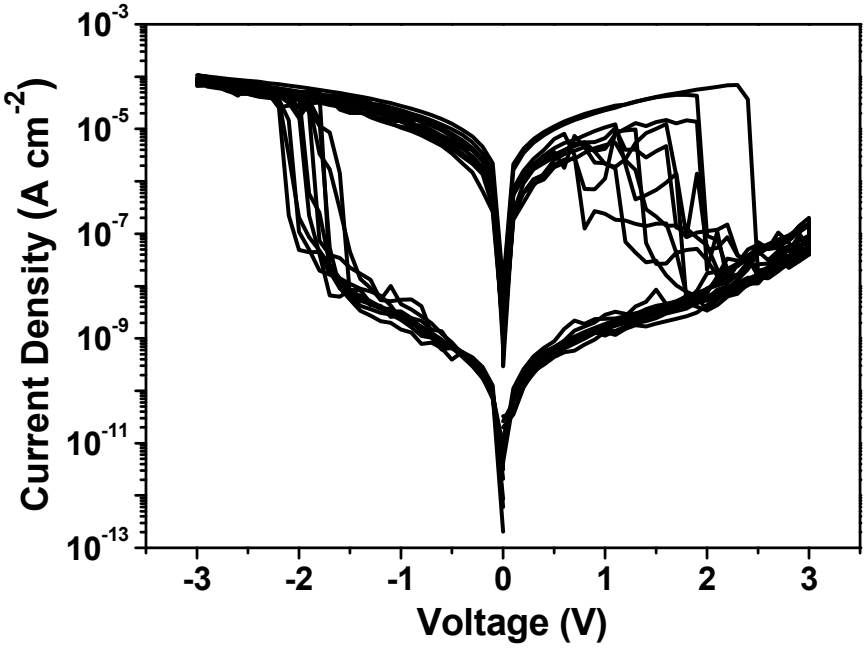

Figure S8. Current density-voltage (*J-V*) characteristic of the flexible **PFT-PI** memory device on successive scan under bending condition (radius of curvature: 30 mm).

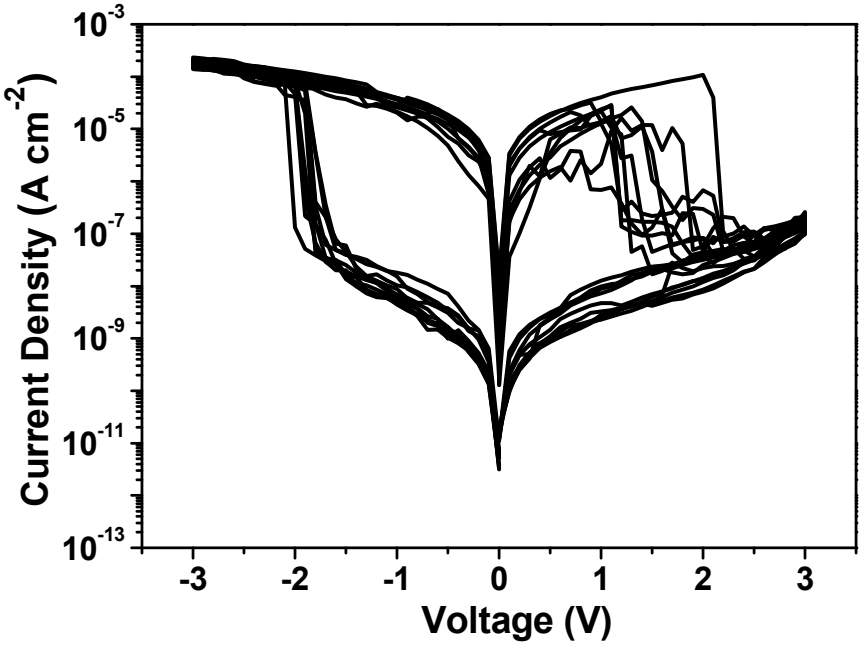

Figure S9. Current density-voltage (*J*-*V*) characteristic of the flexible **PFT-PI** memory device on successive scan under bending condition (radius of curvature: 20 mm).

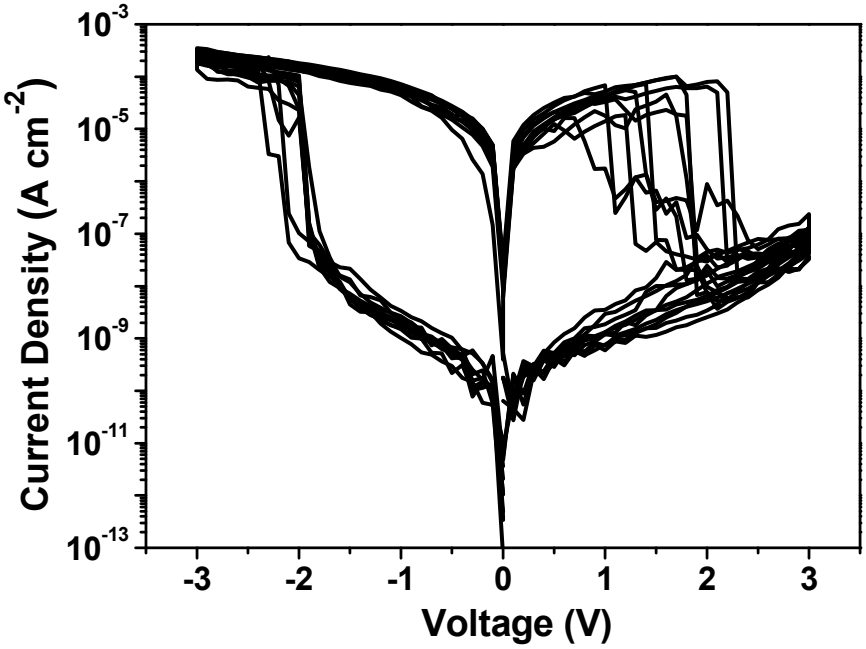

Figure S10. Current density-voltage (*J*-*V*) characteristic of the flexible **PFT-PI** memory device on successive scan under bending condition (radius of curvature: 10 mm).

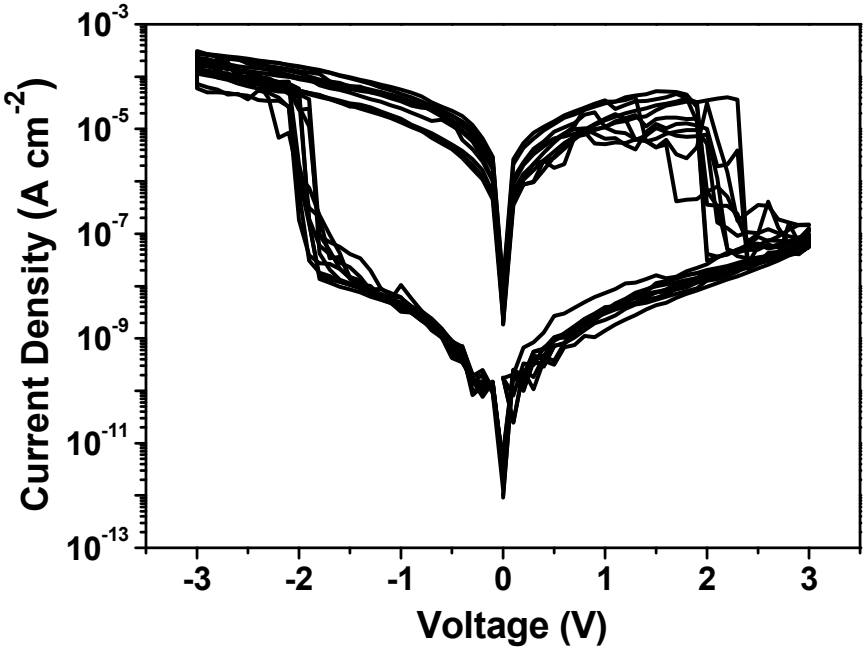

Figure S11. Current density-voltage (*J*-*V*) characteristic of the flexible **PFT-PI** memory device on successive scan under bending condition (radius of curvature: 5 mm).

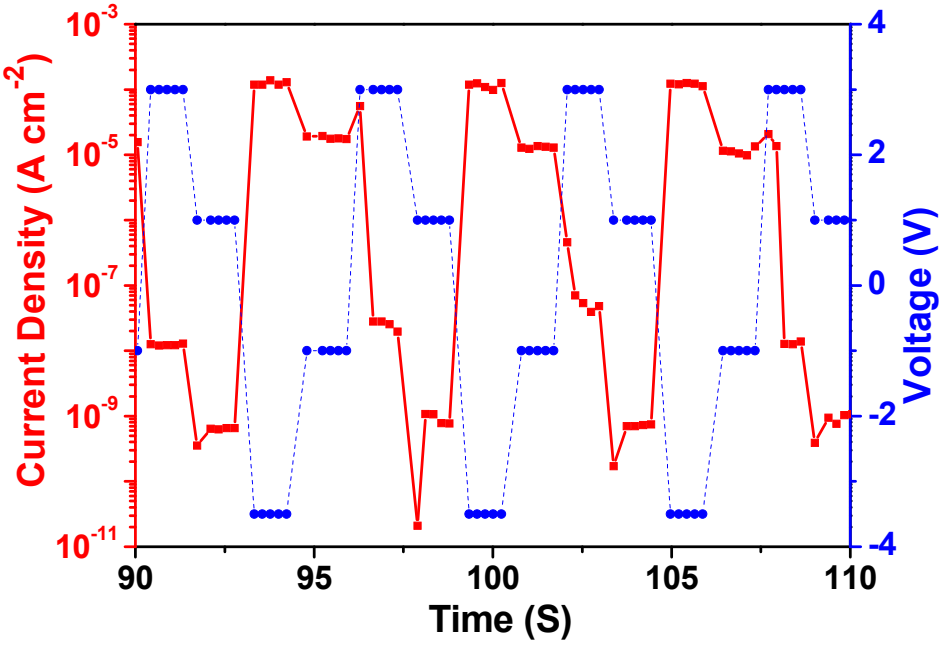

Figure S12. WRER cycles of **PFT-PI** memory device.

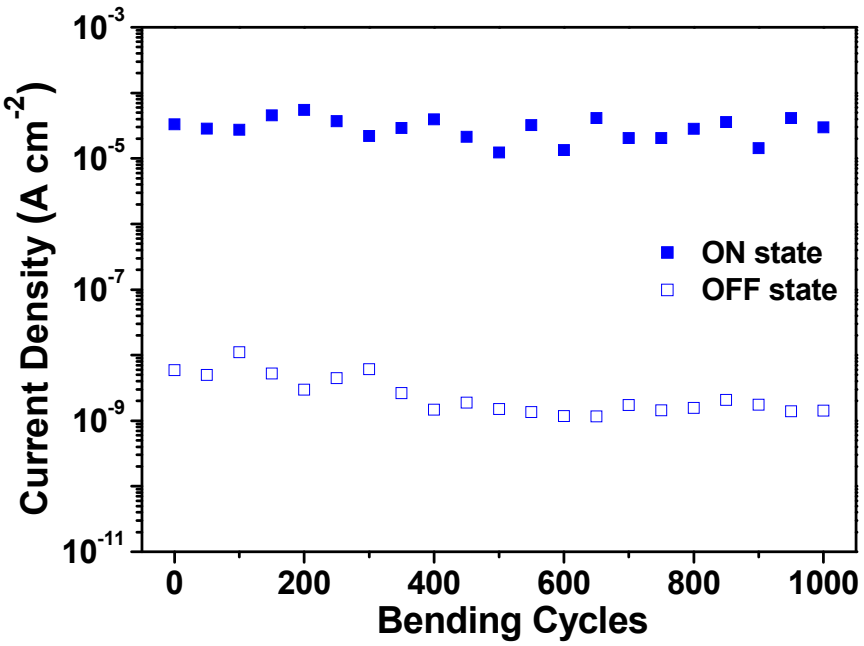

Figure S13. Mechanical endurance of the flexible **PFT-PI** memory device.

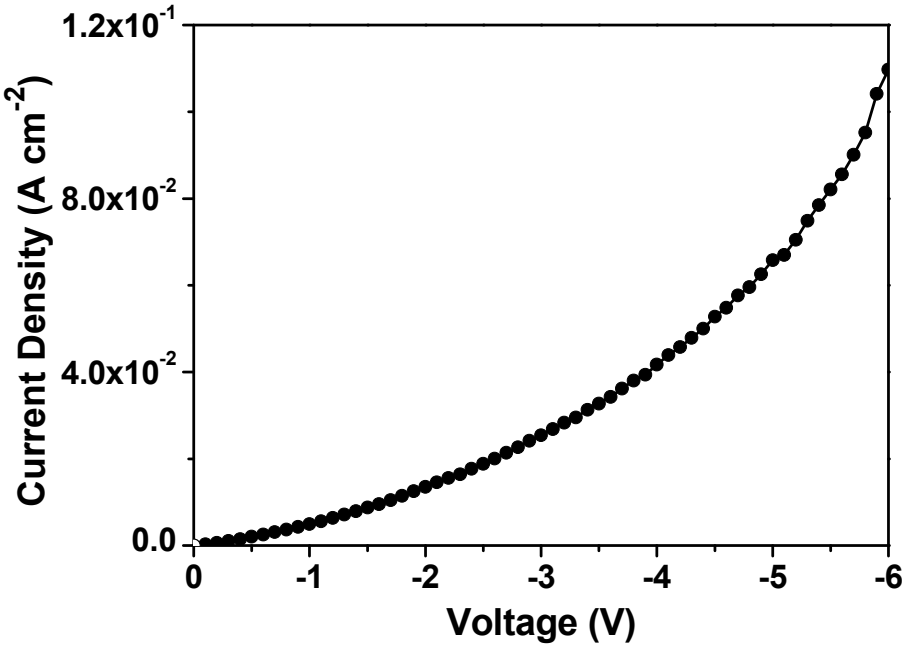

Figure S14. *J-V* characteristics of the **PFT** device.

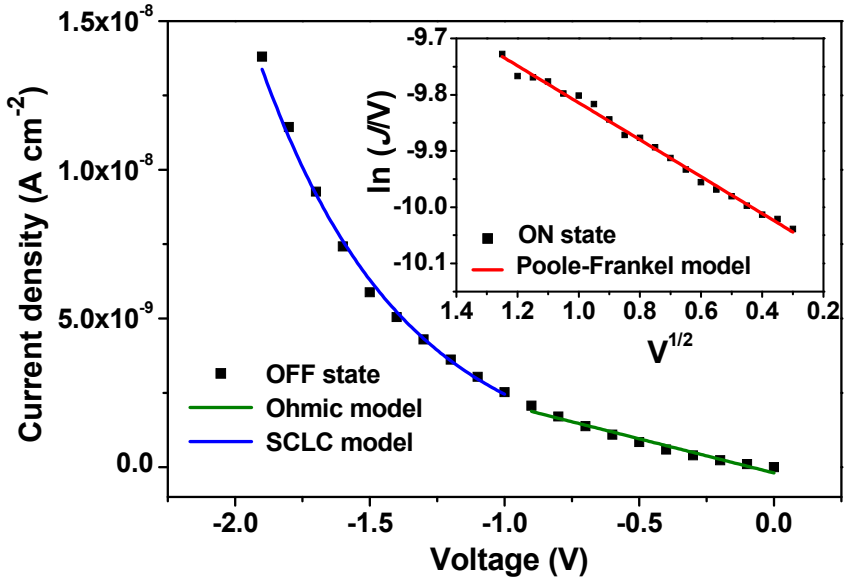

Figure S15. Experimental and fitted *J-V* characteristics of **PFT-PI** device in the OFF and ON states.

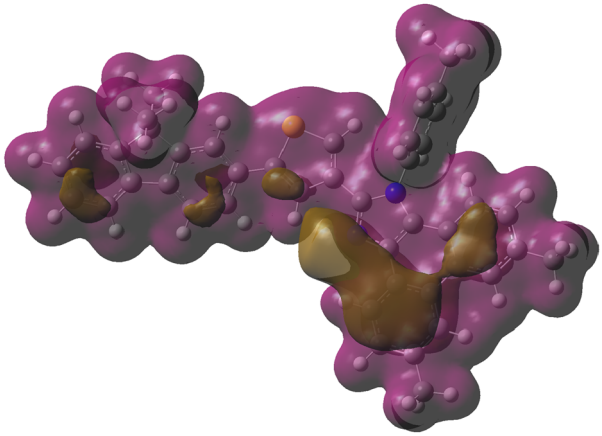

Figure S16. ESP surface of **PFT-PI**.